

Evaluation of Shear Modulus and Damping in Dynamic Centrifuge Tests

A. J. Brennan¹; N. I. Thusyanthan²; and S. P. G. Madabhushi³

Abstract: Correct evaluation of shear modulus and damping characteristics in soils under dynamic loading is key to both the fundamental understanding of soil behavior and the practical application of soil modeling programs. Dynamic centrifuge tests can contribute significant information about soil behavior, but great care must be taken over the signal processing techniques involved, and the test conditions are different from the laboratory experiments that form the database of existing knowledge. This paper outlines several factors that require careful consideration when deriving stiffness and damping parameters from centrifuge data. Shear modulus and damping degradation curves for a dry sand, saturated sand, soft clay and a model waste are then evaluated to explore some of the factors that are introduced during centrifuge tests. Stiffness is seen to be a more reliable parameter than damping ratio. Damping during centrifuge tests for certain materials appeared to differ from the expected values.

DOI: XXXX

CE Database subject headings: Shear; Damping; Soil dynamics; Sand; Clays; Municipal wastes; Centrifuge.

Introduction

The cyclic shear stress–shear strain behavior of soils is key to an understanding of how sites will respond to applied shear loads such as those created by an earthquake. This is nonlinear and hysteretic. Numerical soil models use the variation of shear modulus and damping with strain level, $G-\gamma$ and $D-\gamma$ curves, as fundamental input parameters for dynamic analyses. These would ordinarily be based on element tests carried out, either on the specific material in question or on representative similar materials published in the literature.

Dynamic centrifuge testing represents an alternative technique for investigating soil behavior. As real soil is used, there is no dependence on model parameter values, and stresses and strains are transferred without the confines of an element test. However, data may only be obtained as a time series of values recorded by available instrumentation at specific points. Instrumentation and data acquisition quality provide the constraints. This paper will present a simple technique for using centrifuge accelerometer data to determine both shear modulus and damping in soils undergoing base shaking at multiple input frequencies. Backcalculation of damping in particular is a largely unexplored area. Several important considerations in handling data are discussed. A selection of centrifuge data from a variety of soils will then be

used to compare values obtained with those in previously published data/design curves, to investigate the effects of centrifuging on modulus and damping. The scaling associated with centrifuge testing at N times earth's gravity recreates prototype stress and strain, but other factors are also changed. In particular the frequency of dynamic events is N times faster, which could have an effect on the soil response.

Shear Moduli and Damping in Soils

The relative importance of parameters affecting shear modulus and damping were summarized by Hardin and Drnevich (1972b). Shear strain amplitude, effective stress level and void ratio were listed as affecting shear modulus most in clean sands. Damping was considered to be affected by these too, with number of loading cycles also being a major factor. For clays, the number of loading cycles has been correlated to a decrease in shear modulus with associated pore pressure increase, as summarized by Idriss et al. (1978). Overconsolidation ratio and plasticity index are also influential in clay behavior.

Many studies have used cyclic triaxial or resonant column tests to determine these parameters as functions of shear strain and effective stress for various materials, for example, gravels (Seed et al. 1986; Rollins et al. 1998), sands (Wilson 1988; Kokusho 1980), loess (Hardcastle and Sharma 1998), and clays (Idriss et al. 1978; Kokusho et al. 1982; Vucetic and Dobry 1991). Field studies have also been carried out to investigate stiffness nonlinearity, based on earthquake motions (Chang et al. 1989; Zeghal and Elgamal 1994; Zeghal et al. 1995). Such fieldwork can unfortunately only occur on the few instrumented sites. Centrifuge testing avoids the limitations in soil type available in a field test, and the physical constraints of an element test.

It is not usual to see centrifuge data used to develop stress–strain loops, or derive stiffness and damping parameters. Koga and Matsuo (1990) derived stress strain loops in 1 g shaking table models to describe liquefaction effects. Ellis et al. (1998) derive modulus and damping of very dense sand saturated with different

¹Junior Research Fellow, Engineering Dept., Schofield Centre, Cambridge Univ., Trumpington St., Cambridge CB2 1PZ, UK.

²Research Student, Engineering Dept., Schofield Centre, Cambridge Univ., Trumpington St., Cambridge CB2 1PZ, UK.

³Senior Lecturer, Engineering Dept., Schofield Centre, Cambridge Univ., Trumpington St., Cambridge CB2 1PZ, UK.

Note. Discussion open until May 1, 2006. Separate discussions must be submitted for individual papers. To extend the closing date by one month, a written request must be filed with the ASCE Managing Editor. The manuscript for this paper was submitted for review and possible publication on October 1, 2004; approved on May 6, 2005. This paper is part of the *Journal of Geotechnical and Geoenvironmental Engineering*, Vol. 131, No. 12, December 1, 2005. ©ASCE, ISSN 1090-0241/2005/12-1-XXXX/\$25.00.

pore fluids based on centrifuge work carried out in Japan. Zeghal et al. (1999) used stress-strain loops when looking at dry sand response during earthquakes. Teymur and Madabhushi (2002) generated stress-strain loops to exemplify wavelet techniques and describe boundary effects in centrifuge packages. Ptilakis et al. (2004) plotted some first order loops to compare centrifuge and numerical data. Arulnathan et al. (2000) and Ghosh and Madabhushi (2002) backcalculated G_{\max} from measured shear wave velocities using air-hammer devices. With centrifuge testing, there is an added complication of scaling laws. Important issues to bear in mind here are the use of viscous pore fluids to match seepage and dynamic time scales, and the increased loading frequencies that must be used to represent lower prototype frequencies.

Data Handling

Data described here are obtained from centrifuge tests, where accelerometers are typically arranged in columns containing between three and six instruments. Accelerations \ddot{u} are obtained from which parameters must be inferred. The instruments used in this work are D. J. Birchall type A/23 charge-based accelerometers. Response characteristics of accelerometers obviously vary between make and model, but these particular instruments have a poor response at low frequencies (-3 dB at 4 Hz) which has implications when performing numerical integration. Demonstrative examples shown in this section are from three accelerometers aligned vertically in a dense/medium dense level bed of dry Hostun S28 sand, described further by Ptilakis et al. (2004). Recorded accelerations by instrument number i at depth z_i are written as $\ddot{u}_i [= \ddot{u}(z_i)]$.

Calculation of Shear Stress

From the original shear beam equation, shear stress τ at any depth z may be written as the integration of density ρ times acceleration \ddot{u} through higher levels.

$$\tau(z) = \int_0^z \rho \ddot{u} dz \quad (1)$$

The equations proposed by Zeghal and Elgamal (1994) for field measurements utilize acceleration measured at the surface as they deal with site data. In contrast, a reliable surface acceleration is rarely available in centrifuge testing as the instrument needs to be buried to maintain good contact with the soil. A linear fit is therefore recommended between adjacent pairs of instruments, which may be extrapolated from the top pair to the surface

$$\ddot{u}(z) = \ddot{u}_1 + \frac{(\ddot{u}_2 - \ddot{u}_1)}{(z_2 - z_1)}(z - z_1) \quad (2)$$

If many accelerometers are present, and significant amplification/attenuation is observed, a trapezoidal integration can be used to obtain shear stress. In many centrifuge tests, neither apply. Therefore shear stress is evaluated using Zeghal and Elgamal's expression with the interpolated surface acceleration obtained from Eq. (2) with $z=0$:

$$\tau(z) = \frac{1}{2} \rho z (\ddot{u}(0) + \ddot{u}(z)) \quad (3)$$

Direct integration of the linear approximation for \ddot{u} [Eq. (2)] may also be applied to obtain the same result. The following equation demonstrates this for shear stress at depth z_2 :

$$\tau(z_2) = \frac{1}{2} \rho \frac{[\ddot{u}z_2^2 + \ddot{u}_2 z_2(z_2 - 2z_1)]}{(z_2 - z_1)} \quad (4)$$

For these expressions to apply, adjacent accelerometers must be within a half-wavelength or "spatial aliasing" can occur. If accelerometers are spaced at 100 mm intervals, wavelengths under 200 mm are at risk of this. At an example shear wave velocity $V_s=160$ m/s, this would affect frequencies in excess of 800 Hz, and is not an issue for the data presented in this paper.

Calculation of Shear Strain

Two methods of shear strain calculation are available, a first or a second order expression. Displacement must first be obtained from the acceleration recordings. Recorded data used for this work contained about 0.15 s of data prior to the start of shaking, and a certain amount of time after shaking has stopped, in which noise and ambient vibration is present. It is possible to cut these parts from the signal prior to processing. However the effects of filtering (see the following text) can introduce unwanted errors if the extreme ends of the data signal are nonzero, as the filter is effectively being applied to a step function. Therefore it is safer to leave these extraneous datapoints present, and to force them to equal zero while there is no shaking. This will prevent the noise being integrated to produce finite displacements before loading, and also prevent the filter-induced perturbations interfering with the signal.

Acceleration data must be band-filtered prior to integration (see the following text) to produce velocity, and then filtered *again* before being integrated to displacement u . This is important as low frequency information present in the velocity trace is common, and produces a characteristic linearly varying displacement that continues changing after the end of shaking.

If only two instruments are present in a given soil layer, as would be common when testing soil conditions that change with depth or instrument malfunction is experienced, a simple first order approximation must be applied

$$\gamma = \frac{(u_2 - u_1)}{(z_2 - z_1)} \quad (5)$$

This applies for any point between instruments 1 and 2, and as such is more appropriate for the midpoint.

If three instruments are stacked in a soil column then a better, second order approximation may be made:

$$\gamma(z_i) = \left[(u_{i+1} - u_i) \frac{(z_i - z_{i-1})}{(z_{i+1} - z_i)} + (u_i - u_{i-1}) \frac{(z_{i+1} - z_i)}{(z_i - z_{i-1})} \right] / (z_{i+1} - z_{i-1}) \quad (6)$$

This would apply at depth z_i . Eq. (6) is also part of the Zeghal and Elgamal work.

Calculation of Shear Modulus

Having obtained shear stress and shear strain, a plot of one against the other enables evaluation of shear modulus. A reliable

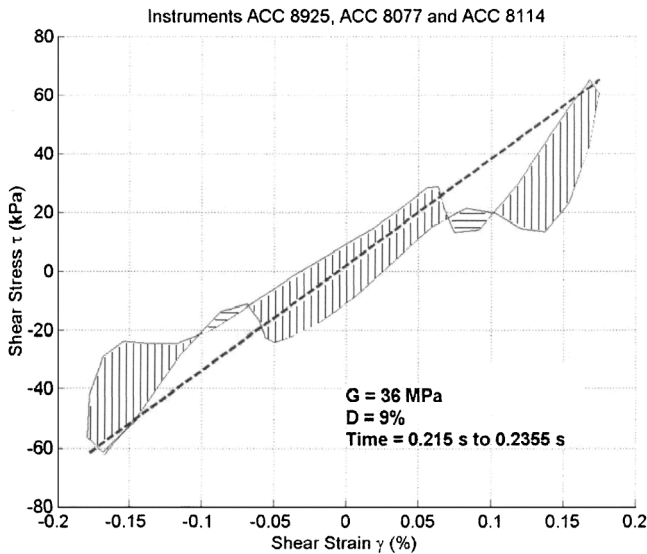


Fig. 1. Stress–strain loop for a particular multifrequency loading of dry sand

method must be found for finding representative slopes through loops such as the one illustrated in Fig. 1, where higher frequency loading components affect the curve and produce many tangent changes. The most reliable method of producing representative moduli has been to evaluate the difference in maximum and minimum stress applied during a loop, and the difference in maximum and minimum strain developed in that loop. The ratio of these two values has been used throughout for shear modulus calculation, and is plotted as a dashed line on Fig. 1.

To compare measured shear moduli with standard degradation curves also requires a value for the small-strain shear modulus G_{\max} against which shear modulus is usually normalized. Test data shown below is normalized by a G_{\max} obtained from

$$G_{\max} = V_s^2 \rho \quad (7)$$

where V_s = shear wave velocity and ρ = soil density. For the model waste and the saturated sand, shear wave velocity V_s is obtained using a miniature air hammer which operates at strains around 0.03% (Ghosh and Madabhushi 2002). For the dry sand and the clay no such data was available. V_s for the clay is estimated from signals in a small earthquake ($\gamma \sim 0.3\%$). It would be expected that the value of G_{\max} obtained this way would be less than the actual value due to the increased strains. In the dry sand, waves traveled too quickly to allow an accurate estimate of time lag to be made. The natural frequency of the soil layer f_0 was obtained from the calculated transfer function, and shear wave velocity estimated using

$$V_s = 4Hf_0 \quad (8)$$

in which H = soil layer thickness. When cross checked against each other, the methods produced comparable values. Clearly the air hammer is the preferred method if available.

Calculation of Equivalent Damping Ratio

It is rare to find estimation of damping values from acceleration records in the literature. Data such as that from Abdel-Ghaffar and Scott (1979) has been based on heavily filtered data that leave nice clean ellipses whose areas may readily be calculated. Data

from laboratory tests have been based on true single frequency loading so areas may also be calculated easily. For evaluation of damping during centrifuge experiments it must be remembered that actual loading frequencies are many times the frequency being interpreted (here, 50+ times greater), and also many times larger than frequencies commonly used in element testing.

Backcalculation of damping is performed at the stress–strain loop stage. A simple trapezoidal integration between datapoints is used to estimate the area inside the bounds of the loop representing work done W . Fig. 1 shows a potential source of error. High frequency components of loading, which are not noise but actual stresses applied by the actuator, cause the loop to cross itself. This is seen in the small regions shaded with horizontal bars in Fig. 1, at about 0.08 and -0.08% shear strain. The net effect of these upon integration is negative; work *appears* to be released by the system rather than absorbed. Such energy changes are unlikely in reality, and the crossover areas must be generated by the applied multifrequency loading path. The contribution of these crossover areas have been taken as a guide to the accuracy of any given damping estimate in a loop. The rare loops with significant crossover are considered unrepresentative. A *net* negative damping for a complete loop (as might be produced if one of the instruments has malfunctioned) is impossible as this contravenes the second law of thermodynamics.

The equivalent damping ratio is defined in the conventional way,

$$D = \frac{1}{2\pi} \frac{W}{W_{elastic}} = \frac{1}{2\pi} \frac{\oint \tau d\gamma}{(0.25 \times \Delta\tau \times \Delta\gamma)} \quad (9)$$

by dividing net work done by 2π times the work that would be retrieved if the system was elastic with stiffness G . It is evaluated by taking $\frac{1}{4}$ times the total stress range $\Delta\tau$ times the total strain range $\Delta\gamma$.

Thus damping is calculated using the area of the actual stress–strain loop.

Appropriate Data Filtering

It is important to filter data at high frequency to eliminate noise and at low frequency to eliminate drift errors during integration. Unlike many laboratory experiments, the loading applied by a centrifuge earthquake actuator is not necessarily single frequency. Higher harmonics of the main shaking frequency can exist, that are real loading components and not noise. Therefore their presence affects the response and they should not be filtered out. Also, earthquake actuators are increasingly being made to apply multifrequency loading, such as those at UC Davis and RPI in the United States and HKUST in Hong Kong.

The purpose of this section is to illustrate the effects of inappropriate filtering, quantified with a specific example. Variations in equipment between institutions will naturally affect error magnitude and choice of filtering frequency. Results presented in this paper are based on data filtered with an FIR digital filter of order 512 using a Hamming window. The *MATLAB* (copyright The MathWorks Inc.) command `filtfilt` is used to eliminate phase distortion.

Fig. 2 shows an input acceleration and Fourier spectra for the signal (unfiltered) used to create the loops in Figs. 1, 3, and 4. It can be seen that in addition to the main driving frequency of 50 Hz, significant harmonics are present at 150, 250, and even

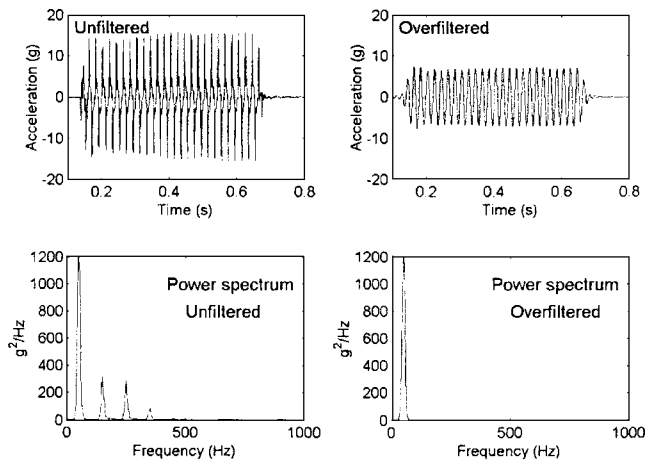


Fig. 2. Frequencies present in a typical motion, and the effects of overfiltering data

350 Hz. Filtering was performed at 20–450 Hz to produce Fig. 1. The effect of not filtering at all on the stress–strain loop is shown in Fig. 3.

By not filtering it is seen that the strain axis in particular is completely wrong as low-frequency drift has caused the signal to walk away from the zero strain origin. The calculated shear modulus is too low as the strain range appears larger than it should due to superimposed drift. Calculated damping is nonsensical as the loop does not close.

This much is well understood, but more common are loops such as Fig. 4, which has been produced by applying a bandpass filter between 20 and 70 Hz to the same data shown in Fig. 1. Only the first harmonic of shaking frequency remains. By filtering out the higher harmonics the loop appears closer to those published as a result of laboratory tests, where single frequency vibration has really been applied, and create a very nice picture. No “walking” errors are experienced as the low frequencies have been eliminated. However, elimination of higher frequency components removes the detail of the actual load path, and increases the calculated damping. The loop in Fig. 4 is fatter than that in

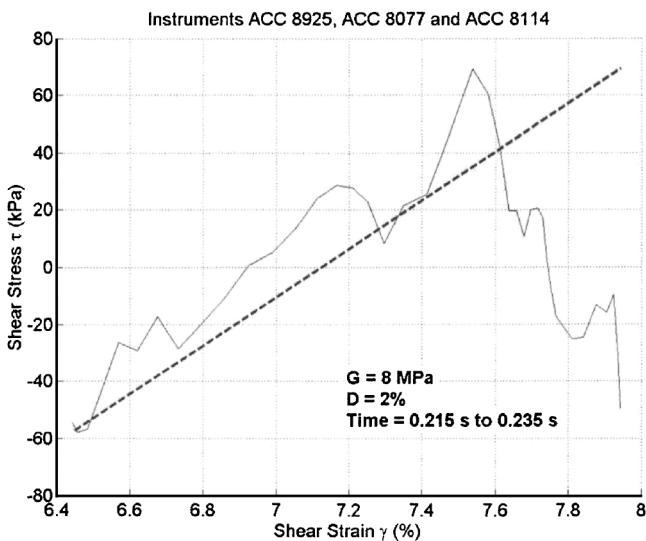


Fig. 3. “Walking” errors associated with unfiltered low frequency accelerometer drift

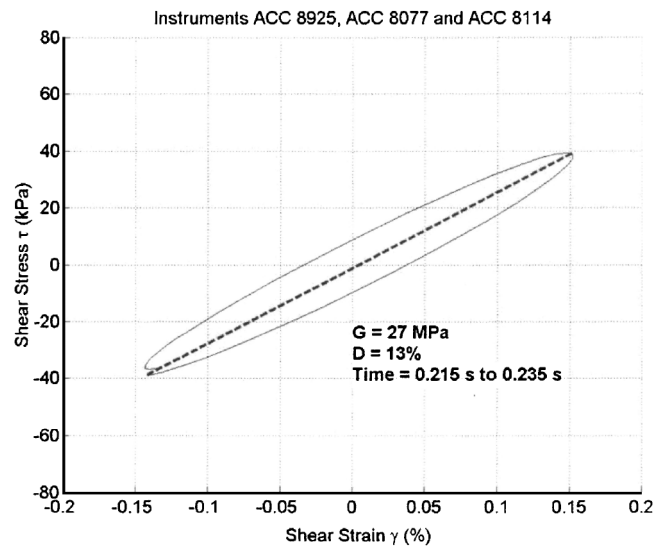


Fig. 4. Incorrect, overfiltered stress–strain loop for the data in Figs. 1 and 2

Fig. 1; 8% damping appeared to increase to 13%. Also removed is the detail of the sharpness at the stress peak. Peak stress in Fig. 4 is reduced from the 65 kPa (Figs. 1 and 3) to about 39 kPa and the crest is rounded off, and therefore a corresponding decrease in recorded shear modulus is experienced (36 MPa reduced to 25 MPa). Fig. 2 shows the time trace of this signal and its Fourier spectrum, which is clearly somewhat distorted from the loads that have really been applied. This is incorrect, because real data has been removed.

High frequency data may also be present in the soil response. Fig. 5 shows the method as applied to saturated sand. The stress–strain response is shown for several loading cycles, after the first two cycles have already passed, generating significant excess pore pressures. Stiffness is considerably reduced except when large strain is applied in which case the soil begins to dilate and a sudden stiffening is seen. After the large stress cycle, however, the soil has become too soft and is not transmitting shear waves

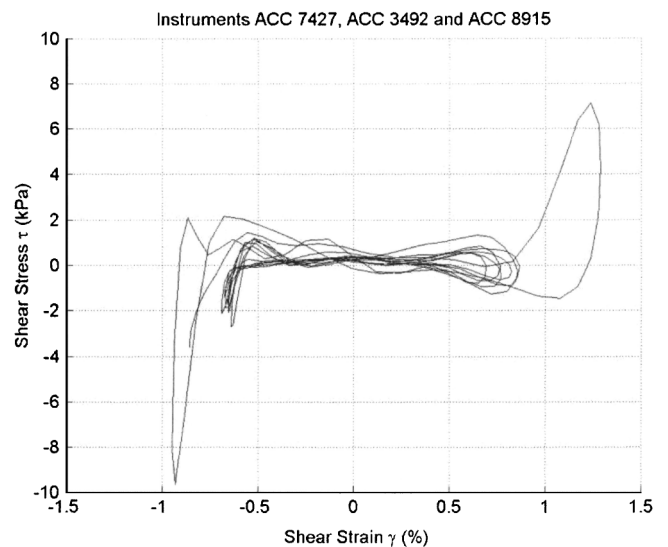


Fig. 5. High frequency components generated by soil response; here through dilation

Table 1. Properties of Materials Investigated

	Dry sand	Saturated sand	Clay	Model waste
Specification	Hostun S28	Fraction E	E-grade kaolin	Peat/sand/clay
Pore fluid	None	50 cSt silicone oil	Water	Water
Density (kg/m ³)	1,600	1,900	1,660	1,000
Voids ratio	0.68	0.80	1.45	2.26
Moisture content	0%	30%	55%	23%
D_{50} (μm)	150	140	5	380
V_s (m/s)	200	145–170	70	70
Permeability (m/s)	N/A	10 ⁻⁴	5 × 10 ⁻⁸	N/A
Plasticity index	0	0	21	0

significantly anymore. This dilation effect creates high frequencies in the soil that are not present in the applied loads. The secant shear modulus calculated now appears to be a nonsensical value (of 0.75 MPa) whereas in fact two distinct stiffnesses are seen during the loading cycle.

Actual filtering frequencies used are of course totally dependant on the spectrum of input motion, as is the magnitude of error derived from excessive filtering.

Shear Modulus from Centrifuge Tests

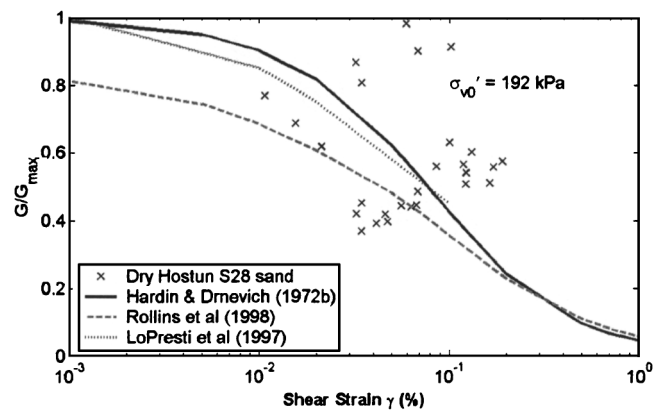
In this section, the method described will be applied to evaluate shear modulus degradation curves from centrifuge tests on four different geotechnical materials, summarized in Table 1.

All tests described have been carried out at 50 g on the Cambridge 10 m diameter beam centrifuge (Schofield 1980). Earthquake motion is applied using the mechanical stored angular momentum actuator described by Madabhushi et al. (1998), for which a typical input motion would be as in Fig. 2. Between 15 and 25 cycles are usually applied, at target frequencies from 30 to 50 Hz (modeling prototype earthquakes between 0.6 and 1 Hz). Harmonics of input frequency are generated by the mechanical system (as in Fig. 1) and other higher frequency data may be generated by soil response (as in Fig. 5).

Dry Sand

Hostun S28 sand was used in a series of dry tests for the EU-funded NEMISREF project (Pitilakis et al. 2004). This sand is uniformly graded with $D_{50}=0.15$ mm, $e_{min}=0.62$, and $e_{max}=1.01$. Sand was poured dry to a mean voids ratio of $e=0.68$ and a depth of 340 mm. Shear moduli are derived from four accelerometers aligned vertically up the center of the benchmark model. Fig. 6 shows these for the deeper 3 ($\sigma'_{v0}=192$ kPa at the middle instrument) and Fig. 7 shows the shallower 3 ($\sigma'_{v0}=112$ kPa). These are normalized by a G_{max} value of 64 MPa, derived from a shear wave velocity inferred from the soil's natural frequency. Using the expression by Hardin and Drnevich (1972a) gives 119 and 91 MPa instead.

Also plotted on the graphs are curves generated from the equations given by Hardin and Drnevich (1972a) for dry fine sands,

**Fig. 6.** Shear modulus degradation of dry sand, $\sigma'_{v0}=192$ kPa

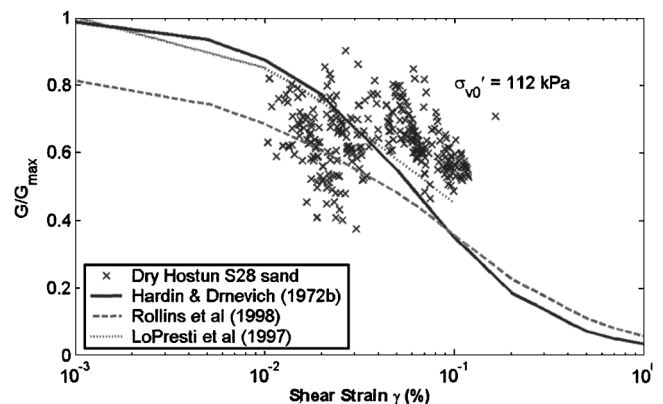
and by Rollins et al. (1998) for gravels, whose best fit curve is also shown to fit data for sands. A best fit through appropriate resonant column data presented by LoPresti et al. (1997) is also plotted.

Both Figs. 6 and 7 show centrifuge data might be representable by the standard curves/element test data, that are a better match at smaller (<0.05%) strains. There is, however, a large degree of scatter, particularly at the higher stress (Fig. 6). This does not correlate with cycle number and must be put down to inherent variability in available measurements. A similar degree of scatter is commonly seen in other test data (Ishibashi and Zhang 1993; Rollins et al. 1998).

Saturated Sand

Fraction E silica sand saturated with silicone oil at 50 cS viscosity was used for a series of centrifuge tests in the work of Brennan (2004). This sand is uniformly graded with $D_{50}=0.14$ mm, $e_{min}=0.61$, and $e_{max}=1.01$. Sand was poured dry to a mean voids ratio of around $e=0.8$, then saturated under vacuum with silicone oil at 50 cS viscosity.

Excess pore pressure build up and the associated acceleration reduction makes shear modulus a harder parameter to obtain from liquefiable sands. Only the first cycle of loading is considered for the data presented, where a clear shear stiffness could be obtained. Stress-strain curves such as that in Fig. 5 are not demonstrating the sort of behavior that can be classified by a stiffness.

**Fig. 7.** Shear modulus degradation of dry sand, $\sigma'_{v0}=112$ kPa

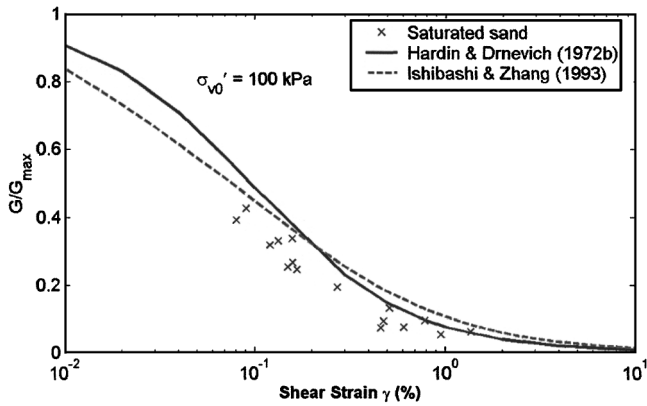


Fig. 8. Shear modulus degradation of saturated sand, $\sigma'_{v0} = 100$ kPa

Fig. 8 shows the data from deeper models, and Fig. 9 data obtained from less deep models. Shear moduli are normalized with respect to G_{max} calculated from shear wave velocity measured in the same sand by Ghosh and Madabhushi (2002). Comparison curves are from Hardin and Drnevich (1972a) and Ishibashi and Zhang (1993).

The centrifuge data are remarkably close to the Hardin and Drnevich curve in both cases. The Ishibashi and Zhang curve is a better fit at the higher effective stress. Interestingly, normalizing data using G_{max} derived from the Hardin and Drnevich equation (66 and 44 MPa) instead of from measured shear wave velocity produces (56 and 40 MPa) a poorer fit. Data in that case lies below the line. That would imply that the shear wave velocity obtained from the air hammer is a reasonable value, and that the Hardin and Drnevich expression for G_{max} is a little too stiff for this case.

Normally Consolidated Clay

E-grade kaolin clay was used in a test carried out by Brennan et al. (2002). The clay is normally consolidated and the pore fluid is water. Three accelerometers are used, with an initial vertical effective stress of 62 kPa at the middle one. Data have been taken from different times during the 15–25 loading cycles of each earthquake to obtain a range of strains. According to experience (e.g., Idriss et al. 1978) shear modulus reduces with number of cycles, possibly if excess pore pressures buildup. However, no

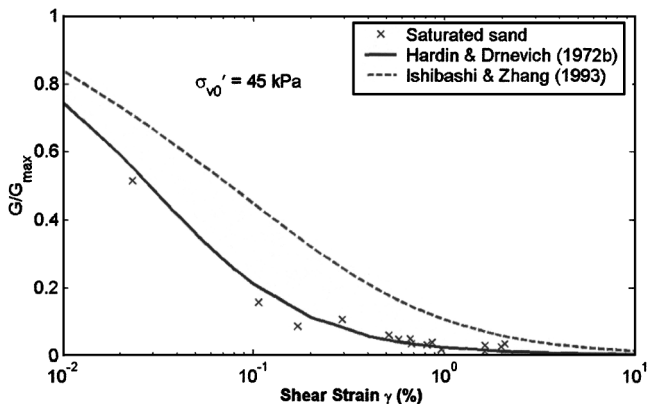


Fig. 9. Shear modulus degradation of saturated sand, $\sigma'_{v0} = 45$ kPa

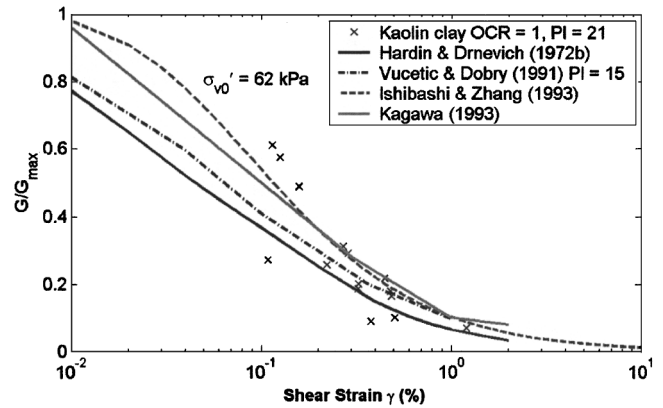


Fig. 10. Shear modulus degradation of normally consolidated clay, $PI = 21$, $\sigma'_{v0} = 62$ kPa

significant pore pressure generation was observed during these experiments, and no correlation was here observed between measured G values and number of cycles. Normalizing parameter G_{max} has been derived from time lags between accelerometers during earthquakes.

Data are plotted in Fig. 10 against the design curves of Hardin and Drnevich (1972a), Vucetic and Dobry (1991), and Ishibashi and Zhang (1993). Also included is a best fit curve through appropriate data from cyclic simple shear and resonant column tests on marine clays reported by Kagawa (1992).

The centrifuge data in Fig. 10 displays the trend and values that would be expected throughout the strain range tested. However, the three points above the line at around 0.1% strain indicate that perhaps the small-strain response is stiffer than would be expected. This may be due to the approximation for G_{max} , 7.5 MPa. The Hardin and Drnevich expression yields 24 MPa which, as with the sands, would have been too stiff.

Model Municipal Solid Waste

An artificial municipal solid waste was produced by Thusyanthan et al. (2004) for investigating the dynamic behavior of landfill systems. A mixture of sand, clay and peat in the mass ratio 1:1:1 was selected, which has static soil parameters representative of real municipal solid waste but none of the associated variability and handling problems. To determine how suitable the dynamic properties of this model material were, the method is applied to recorded accelerometer data as before, and normalized derived shear modulus values are plotted in Fig. 11.

Also plotted are the bounds derived by Augello et al. (1998) by back analyzing five past earthquakes on landfill material, and the bounds derived by Matasovic and Kavazanjian (1998) based on cyclic simple shear tests with back analysis of strong motion data. Matasovic and Kavazanjian had a wide amount of scatter in their test data in the 0.1–10% strain range, but recommend the upper bound for use in practice.

The variable nature of landfill material means that the margins for municipal solid waste (MSW) are a lot wider. However the centrifuge data provides a remarkably good fit, even within the tighter bounds of Augello et al., and closer to the recommended (upper bound) line from Matasovic and Kavazanjian. This close fit strongly supports the use of the model mixture for dynamic modeling of landfill systems.

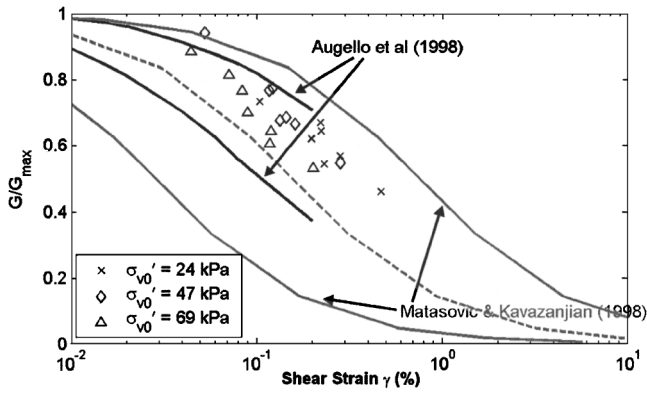


Fig. 11. Shear modulus degradation of a model MSW mix

Equivalent Damping Ratio from Centrifuge Tests

In this section, the method is used to estimate damping values as functions of shear strain during centrifuge model earthquakes. Providing a single suitable loop is chosen containing sufficient datapoints, then a simple numerical integration around the cycle should provide the numerator of Eq. (9). As described above, the loop from which damping is calculated must be representative of hysteretic damping, or the numerical integration will return an inaccurate value, particularly if the stress-strain curve crosses itself in such a way as to subtract from the net result.

Damping has been acknowledged (Hardin and Drnevich 1972b, Teachavorasinskun et al. 2001) to be more affected by loading frequency than shear modulus. This becomes an issue in centrifuge modeling where loading frequencies are necessarily increased to account for the accelerated time scale. Typical loading from an earthquake that would occur at the order of 1 Hz is carried out at 30–100 Hz on the centrifuge, and the shaking device may introduce additional higher frequency loads, so it is important to know which materials will experience this, and to what degree.

Dry Sand

The loops from the dry sand tests described previously are used to generate the damping ratios plotted in Fig. 12. Seed et al. (1986) report that the influence of effective stress is only significant in laboratory tests for very low stresses (<25 kPa), so data from

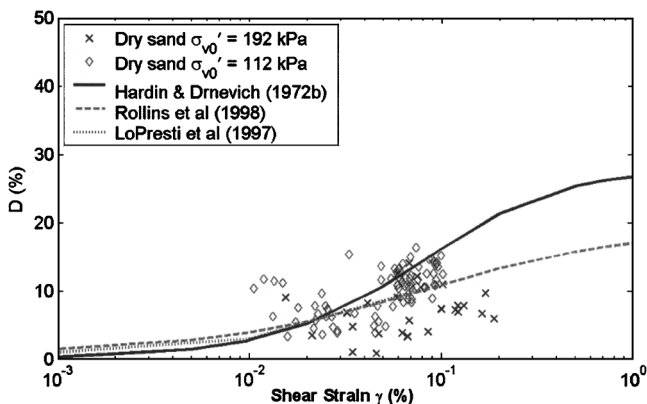


Fig. 12. D - γ relationships for dry sand

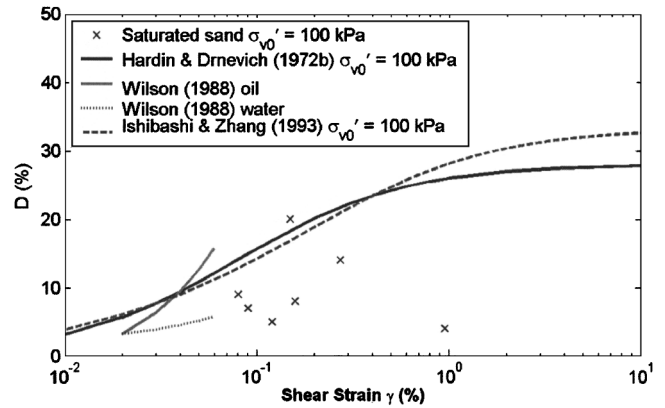


Fig. 13. D - γ relationships for saturated sand, $\sigma'_{v0} = 100$ kPa

both stress levels is plotted on the same axes. Rollins et al. (1998) support this by measuring only a slight reduction in damping (about 2%, strain independent) as stress increases from 50 to 400 kPa. Also in Fig. 12 are curves from the equations of Hardin and Drnevich (1972a) and Rollins et al. (1998).

Data at the higher stress level seem to be on or just below the curve. This sort of scatter is commonly seen in investigations of damping, such as those used to derive the comparative information. At the lower stress level, centrifuge data fits well with the curves; they seem to form reasonable bounds for the data.

Analyses show that the point in the time record (i.e., number of cycles) where the data was obtained does not correlate with damping ratio, unlike other studies (e.g., Kokusho 1980; Hardin and Drnevich 1972b). This perhaps indicates that cycle number has less influence on the hysteretic damping of this particular sand than on those tested in the other studies.

Saturated Sand

Data for saturated sand (test described in Table 1) is plotted in Fig. 13 for the higher stress level and Fig. 14 for the lower stress level. This data are more limited as the calculated damping is not always representative, as described previously. As with the modulus data, only the first cycle of loading is considered due to the buildup of excess pore pressures. Hardin and Drnevich's expression is again used for comparison, along with curves fitted to the data of Wilson (1988) who compared material damping in this

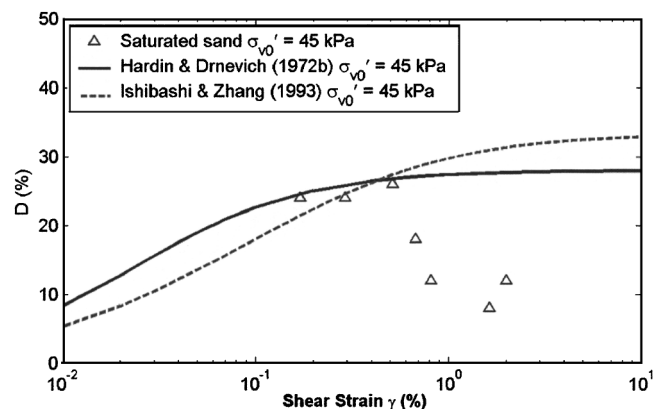


Fig. 14. D - γ relationships for saturated sand, $\sigma'_{v0} = 45$ kPa

same sand saturated with 100 cS silicone oil and with water using a resonant column device, at 100 kPa effective confining pressure.

Wilson's data showing increased damping in the presence of a viscous pore fluid had implications for centrifuge modelers, who are often constrained to use such a fluid for the correct modeling of seepage velocities (e.g., Schofield 1980). But in Fig. 13, the 100 kPa data points around 0.1% strain appear to fall more toward an extrapolation of his water-saturated models than the oil-saturated tests. The mechanism of pore fluid viscosity increasing damping at 1 g could therefore be related to rate of fluid movement through voids. This process is accelerated during centrifuge testing, which is why viscous pore fluid is used in the first place. It would appear as if material damping in centrifuge models should match the prototype providing the correct viscosity is used for the appropriate g-level.

The second interesting point from these plots is the behavior at strains above 0.6%. These data points, which have all come from stress-strain loops deemed to be representative of hysteretic damping, show a marked drop in calculated damping ratio where the value should plateau at a D_{max} . What is probably happening is that by applying such large strains the soil has immediately been taken into a state approaching complete liquefaction. With the soil now operating in a different behavior regime, it appears as if the damping of liquefied soil is much reduced. What are the possible sources for material damping in saturated sand? Frictional energy loss in the soil skeleton is now significantly reduced as the soil particles lose contact with each other. If the pore fluid has hysteretic damping, this should remain constant, depending on how it responds to the associated pressure increase. It would not be expected that this contributes much to the overall damping ratio (Wilson 1988). Fluid-movement induced energy loss will be very much reduced because consolidation coefficient (ratio of permeability to compressibility times unit weight) increases threefold as excess pore pressure ratio increases from approximately 0.6 to 0.95, and goes up to an apparent value approaching 1,000 in liquefied conditions (Brennan 2004).

Obviously the data here is limited in quantity, but it is intriguing that the first-cycle strain required to cause damping to deviate from the expected curves, here around 0.6%, appears more like a cutoff rather than a gradual effect.

Normally Consolidated Clay

E-grade kaolin clay was used to derive the damping data in Fig. 15, along with damping data from the sources used to compare shear modulus previously.

Data collected since the original Hardin and Drnevich work make this equation look like an overprediction, but surprisingly the centrifuge data suggests that the damping obtained during the centrifuge experiment is about 1.5 times the established curves for such material. It would be expected that damping reach an asymptotic value D_{max} at large strains, which is equal to about 28% in Hardin and Drnevich, but rarely do laboratory tests employ sufficiently high strains to achieve such a plateau. Large damping values (up to 45%) have been recorded, by Teachavorasinskun et al. (2001) in cyclic loading tests inducing strains around 10%, for example.

It is widely acknowledged that strain rate has an effect on damping in clayey soils, but this has rarely been quantified. Such a relationship would have implications for dynamic centrifuge testing of soft clay, where applied shaking frequencies are neces-

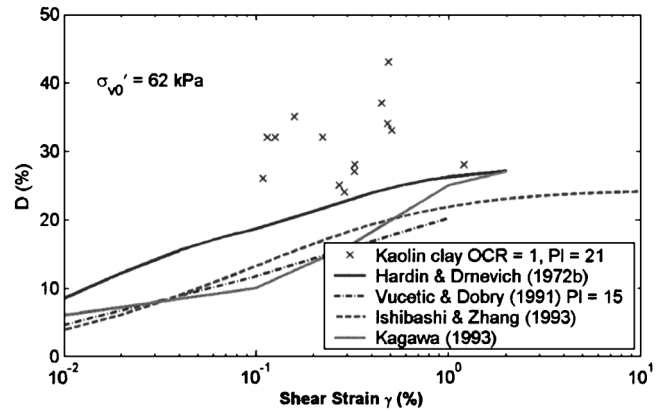


Fig. 15. D - γ relationships for N-C clay, $PI=21$, $\sigma'_{v0}=62$ kPa

sarily tens of times larger than the prototype frequency interpreted. Here, frequencies around 50 Hz are interpreted as being 1 Hz. The only real difference between the centrifuge experiment and the laboratory tests is the shaking frequency. Based on this evidence, it is suggested that dynamic material damping in clays increases by 1.5 times when frequency is increased from 1 to 50 Hz, and as such caution must be exercised when analyzing the results of dynamic centrifuge tests on clayey soils. The effect of this increased hysteretic damping would be a reduction in soil natural frequency and in the response amplitude of surface structures.

Model Municipal Solid Waste

Model MSW was tested to determine whether the damping of this material is representative of real waste. Fig. 16 shows the damping from centrifuge data, along with bounds from Matasovic and Kavazanjian (1998) and Augello et al. (1998) as mentioned previously.

The published bounds surprisingly show mutually exclusive areas, indicating the variability in both landfill material (even from the same site) and in the equivalent damping ratio as a parameter. Centrifuge data provides a good match with the Augello bounds, indicating that the value is representative of a real MSW.

As with previous values from this study, a large degree of scatter is seen. It would appear as if damping ratio as a parameter

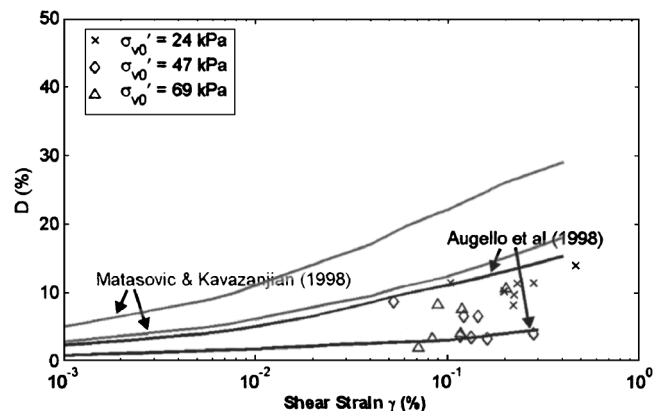


Fig. 16. D - γ relationships for model MSW

cannot be determined any more (or less) accurately by centrifuge testing than alternative methods. Given the wide variability in possible values for this parameter, both in the current study and previous research, it would be advisable that analyses carried out are not strongly influenced by small changes in the input value of damping. This would apply to all soils within the range tested in this paper.

Discussion

Shear modulus values obtained from all centrifuge tests appear to be relatively close to the relevant published degradation curves, with a degree of scatter comparable to that observed in many other investigations. This required the parameter G_{\max} to be obtained from the actual test, as analyses using the Hardin and Drnevich (1972a) equation for small strain stiffness found it to overestimate the soil stiffness. Shear wave velocities obtained from depth averages between data points make a surprising source of good G_{\max} information as even the “small strain” air hammer imparts strains around 0.03%. Being a more reliable parameter than damping, it is perhaps not surprising that existing approximations for $G-\gamma$ curves proved to be suitable for all materials tested here.

The values of damping achieved were subject to more scatter, as might be expected from integrating nonelliptical shape of the traces. It is necessary, though, not to convert figures to equivalent ellipses. The dry sand and the model waste behaved in accordance with the data of other researchers indicating that these materials do not undergo significant parameter changes during centrifuge testing. Saturated sand also behaved as expected, prior to excess pore pressure build up. Testing on saturated samples would ordinarily be performed without the potential for excess pore pressure generation (e.g., dense soils or drained conditions) so this case should match. Post-liquefaction damping behavior has not been investigated by other researchers, and the noticeable reduction measured in these tests has implications for computer codes dealing with such parameters. Further work could quantify the altered damping degradation curves for liquefying sands. Clay did not share damping in common with expected results. This was explained above in terms of the applied shaking frequency.

Earthquake and laboratory test loading frequencies are of the same order of magnitude, around 1 Hz, whereas centrifuge tests at N times earth’s gravity require vibrations to be N times faster. Dynamic centrifuge testing on clayey materials should be interpreted with caution as an excessively large damping ratio could operate. Sands appeared to be unaffected by such frequency effects, in this work.

Conclusions

Centrifuge accelerometer data has been used to produce shear stress-strain loops. Several important considerations have been described to ensure high quality results are obtained. This particularly applies to backcalculation of damping ratios, which have been shown to occasionally suffer from an interesting effect where small anticlockwise loops may be present. These have a negative contribution to calculated damping and if their presence is significant then influences other than material damping are in action. Damping ratios should not be calculated based on “equivalent ellipses” (single frequency motion) if multiple loading frequencies are being dealt with.

Shear modulus values obtained for all materials examined were appropriate when a suitable value for small strain modulus G_{\max} was used, although some degree of scatter was obtained with the dry sand. The value of G_{\max} obtained from the Hardin and Drnevich (1972a) expression was universally too stiff to enable an accurate data fit. Such a value is only required for producing degradation curves anyway, in which case it is recommended to obtain G_{\max} directly from test data if possible.

Equivalent damping ratios obtained were mostly as expected. Judging by the scatter, values obtained were comparable in accuracy and repeatability to alternative methods in use. It would be recommended that analyses utilizing these values not be heavily dependent on a precise damping value. The exceptions were saturated sand, and clay. In saturated sand, excess pore pressure generation at strains above 0.6% caused a sharp reduction in damping compared to the expected values. Backcalculated damping ratios for clays were much higher than expected, by a factor of about 1.5. This is attributed to the higher frequency loading applied on the centrifuge.

Acknowledgments

Centrifuge tests were carried out with the excellent assistance of technical staff at the Schofield Center, Cambridge, which is acknowledged with thanks.

Notation

The following symbols are used in this paper:

D	= equivalent damping ratio;
D_{50}	= sieve size with 50% by mass passing;
e_{\min}, e_{\max}	= minimum and maximum void ratios;
f_0	= fundamental natural frequency;
G	= secant shear modulus
G_{\max}	= maximum (small-strain) shear modulus;
H	= soil layer thickness;
u, \ddot{u}	= horizontal displacement/acceleration;
V_s	= shear wave velocity;
W	= total work done;
W_{elastic}	= equivalent elastic work done;
z	= depth below soil surface;
γ	= strain;
ρ	= bulk density;
σ'_{v0}	= initial vertical effective stress; and
τ	= shear stress.

References

- Abdel-Ghaffar, A. M., and Scott, R. F. (1979). “Shear moduli and damping factors of earth dam.” *J. Geotech. Eng. Div., Am. Soc. Civ. Eng.*, 105(12), 1405–1426.
- Arulnathan, R., Boulanger, R. W., Kutter, B. L., and Sluis, W. K. (2000). “New tool for shear wave velocity measurements in model tests.” *Geotech. Test. J.*, 23(4), 444–453.
- Augello, A. J., Bray, J. D., Abrahamson, N. A., and Seed, R. B. (1998). “Dynamic properties of solid waste based on back-analysis of OII landfill.” *J. Geotech. Geoenviron. Eng.*, 124(3), 211–222.
- Brennan, A. J. (2004). “Vertical drains as a countermeasure to earthquake-induced soil liquefaction.” PhD thesis, Univ. of Cambridge, Cambridge, U.K.
- Brennan, A. J., Madabhushi, S. P. G., and Bolton, M. D. (2002). “Behav-

- ior of a suction caisson in soft clay, under monotonic and earthquake loading." *Rep. to KW Consultants Ltd.*, Cambridge University Technical Services, Cambridge, U.K.
- Chang, C.-Y., Power, M. S., Tang, Y. K., and Mok, C. M. (1989). "Evidence of nonlinear soil response during a moderate earthquake." *Proc., 12th Int. Conf. on Soil Mechanics and Foundation Engineering*, Balkema, Rotterdam, The Netherlands, 1927–1930.
- Ellis, E. A., Soga, K., Bransby, M. F., and Sata, M. (1998). "Effect of pore fluid viscosity on the cyclic behavior of sands." *Proc., Centrifuge 98*, T. Kimura, O. Kusakabe, and J. Takemura, eds., Balkema, Rotterdam, The Netherlands, 217–222.
- Ghosh, B., and Madabhushi, S. P. G. (2002). "An efficient tool for measuring shear wave velocity in the centrifuge." *Proc., Int. Conf. on Physical Modeling in Geotechnics*, R. Phillips, P. J. Guo, and R. Popescu, eds., Balkema, Rotterdam, The Netherlands, 119–124.
- Hardcastle, J. H., and Sharma, S. (1998). "Shear modulus and damping of unsaturated loess." *Geotechnical Earthquake Engineering and Soil Dynamics III, ASCE Geotechnical Special Publication*, 178–188.
- Hardin, B. O., and Drnevich, V. P. (1972a). "Shear modulus and damping in soils." *J. Soil Mech. Found. Div.*, 98(7), 667–692.
- Hardin, B. O., and Drnevich, V. P. (1972b). "Shear modulus and damping in soils: Measurement and parameter effects (Terzaghi Lecture)." *J. Soil Mech. Found. Div.*, 98(6), 603–624.
- Idriss, I. M., Singh, R. D., and Dobry, R. (1978). "Nonlinear behavior of soft clays during cyclic loading." *J. Geotech. Eng. Div., Am. Soc. Civ. Eng.*, 104(12), 1427–1447.
- Ishibashi, I., and Zhang, X. (1993). "Unified dynamic shear moduli and damping ratios of sand and clay." *Soils Found.*, 33(1), 182–191.
- Kagawa, T. (1992). "Moduli and damping factors of soft marine clays." *J. Geotech. Eng.*, 118(9), 1360–1375.
- Koga, Y., and Matsuo, O. (1990). "Shaking table tests of embankments resting on liquefiable sandy ground." *Soils Found.*, 30(4), 162–174.
- Kokusho, T. (1980). "Cyclic triaxial test of dynamic soil properties for wide strain range." *Soils Found.*, 20(2), 45–60.
- Kokusho, T., Yoshida, Y., and Esashi, Y. (1982). "Dynamic properties of soft clay for wide strain range." *Soils Found.*, 22(4), 1–18.
- LoPresti, D. C. F., Jamiolkowski, M., Pallara, O., Cavallaro, A., and Pedroni, S. (1997). "Shear modulus and damping of soils." *Geotechnique*, 47(3), 603–617.
- Madabhushi, S. P. G., Schofield, A. N., and Lesley, S. (1998). "A new stored angular momentum (SAM) based actuator." *Proc., Centrifuge 98*, T. Kimura, O. Kusakabe, and J. Takemura, eds., Balkema, Rotterdam, The Netherlands, 111–116.
- Matasovic, N., and Kavazanjian, E. (1998). "Cyclic characterization of OII landfill solid waste." *J. Geotech. Geoenviron. Eng.*, 124(3), 197–210.
- Pitilakis, K., Kirtas, E., Sextos, A., Bolton, M. D., Madabhushi, S. P. G., and Brennan, A. J. (2004). "Validation by centrifuge testing of numerical simulations for soil-foundation-structure systems." *Proc., 13th World Conf. on Earthquake Engineering*, Vancouver, B.C., Canada, Paper No. 2772.
- Rollins, K. M., Evans, M. D., Diehl, N. B., and Daily, W. D. (1998). "Shear modulus and damping relationships for gravels." *J. Geotech. Geoenviron. Eng.*, 124(5), 396–405.
- Schofield, A. N. (1980). "Cambridge geotechnical centrifuge operations." *Geotechnique*, 30(3), 227–268.
- Seed, H. B., Wong, R. T., Idriss, I. M., and Tokimatsu, K. (1986). "Moduli and damping factors for dynamic analyses of cohesionless soils." *J. Geotech. Eng.*, 112(11), 1016–1032.
- Teachavorasinskun, S., Thongchim, P., and Lukkunaprasit, P. (2001). "Shear modulus and damping ratio of a clay during undrained cyclic loading." *Geotechnique*, 51(5), 467–470.
- Teymur, B., and Madabhushi, S. P. G. (2002). "Shear stress-strain analysis of sand in ESB model container by harmonic wavelet techniques." *Proc., Int. Conf. on Physical Modeling in Geotechnics*, R. Phillips, P. J. Guo, and R. Popescu, eds., Balkema, Rotterdam, The Netherlands, 201–206.
- Thusyanthan, I., Madabhushi, S. P. G., and Singh, S. (2004). "Modeling the seismic behavior of municipal solid waste." *Proc., 11th Int. Conf. on Soil Dynamics and Earthquake Engineering/3rd Int. Conf. on Earthquake Geotechnical Engineering*, D. Doolin, A. Kammerer, T. Nogami, R. B. Seed, and I. Towhata, eds., Univ. of California, Berkeley, Calif., 2, 283–290.
- Vucetic, M., and Dobry, R. (1991). "Effect of soil plasticity on cyclic response." *J. Geotech. Eng.*, 117(1), 89–107.
- Wilson, J. M. R. (1988). "A theoretical and experimental investigation into the dynamic behavior of soils." PhD thesis, Univ. of Cambridge, Cambridge, U.K.
- Zeghal, M., and Elgamal, A.-W. (1994). "Analysis of site liquefaction using earthquake records." *J. Geotech. Eng.*, 120(6), 996–1017.
- Zeghal, M., Elgamal, A.-W., Tang, H. T., and Stepp, J. C. (1995). "Lotung downhole array. II: Evaluation of soil nonlinear properties." *J. Geotech. Eng.*, 121(4), 363–378.
- Zeghal, M., Elgamal, A. W., Zeng, X., and Arulmoli, K. (1999). "Mechanism of liquefaction response in sand-silt dynamic centrifuge tests." *Soil Dyn. Earthquake Eng.*, 18(1), 71–85.